

Crack Front Waves and the dynamics of a rapidly moving crack

E. Sharon¹, G. Cohen², and J. Fineberg²

¹The Center for Nonlinear Dynamics, The University of Texas, Austin 78712, TX, USA

²The Racah Institute of Physics, The Hebrew University of Jerusalem, Jerusalem 91904, Israel

Crack front waves are localized waves that propagate along the leading edge of a crack. They are generated by the interaction of a crack with a localized material inhomogeneity. We show that front waves are nonlinear entities that transport energy, generate surface structure and lead to localized velocity fluctuations. Their existence locally imparts inertia, which is not incorporated in current theories of fracture, to initially “massless” cracks. This, coupled to crack instabilities, yields both inhomogeneity and scaling behavior within fracture surface structure.

PACS numbers:46.50.+a, 62.20.Mk, 68.35.Ct

Dynamic fracture is of fundamental and practical importance. We consider the behavior of a crack interacting with a localized defect. We shall show that this interaction can induce fundamental changes to a crack’s long-term dynamics. These changes imply that a necessarily 3D view of fracture must replace the basically 2D theory that is currently used to describe fracture in ideal materials.

In ideal (defect-free), brittle amorphous materials, experiments [1–3] indicate that until a crack bifurcates, its dynamic behavior is in excellent agreement with an equation of motion [4,5] based on a linear elastic description of a moving crack in a 2D material. Balancing the energy flux, G , per unit length of the crack with the fracture energy, Γ , defined as the energy needed to create a length of new fracture surface yields:

$$G(v, l) \sim G(l)(1 - v/v_R) = \Gamma \quad (1)$$

where v and v_R are, respectively, the instantaneous crack velocity and the Rayleigh wave speed of the material. $G(l)$ is dependent solely on the instantaneous crack length, l , and the loading conditions. As Eq. (1) has no inertial terms, a crack tip in a 2D material should behave as a massless, point-like object. In ideal materials, Eq. (1) was shown [2] to break down when, beyond a critical velocity, v_c , a single crack loses stability [6–8] to a state in which a crack undergoes repetitive, short-lived microscopic branching (“micro-branching”) events (see e.g. [9]).

Let us now consider the dynamics of a crack in a “non-ideal” material populated by asperities (i.e. defects which locally perturb Γ). When a crack encounters an asperity, the system’s translational invariance normal to the propagation direction (z axis in Figure 1a) is broken. Thus, a crack tip can no longer be idealized as a pointlike object propagating within an, effectively, 2D material. The

dynamics of the 1D front defined by the leading edge of the crack in a 3D material must now be considered. In this Letter we will demonstrate that localized waves, “front waves”, generated by an asperity, fundamentally affect a crack’s dynamics. Front waves (FW) are elastic waves that propagate along a moving crack front. We will show that these waves both transport energy along the crack front and locally impart inertia to the initially “massless” crack. This leads to a sharp localization of the energy flux at points along the front as well as both self-perpetuating inhomogeneities and scaling of the fracture surface structure.

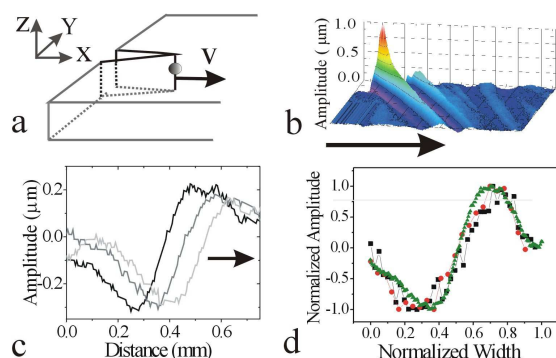


FIG. 1. (a) The translational symmetry along a crack front (z direction) is broken when the front (propagating in the x direction) encounters a localized asperity. (b) The interaction with a single asperity (located at the origin) produces localized front waves (FW) that propagate along the front while generating tracks on the fracture surface. Shown is a fracture surface scan of a 1.5mm x 1.5mm section of the xz plane. (c) 3 sequential profiles in the xy plane showing FW form and motion. (Time increases in direction of arrow.) (d) FW have a unique characteristic profile. Shown are 3 different FW whose width was normalized by the spatial scale, W , of the initial asperity: $W = 130\mu\text{m}$ (\square) $205\mu\text{m}$ (\circ) and $445\mu\text{m}$ (\triangle). Arrows indicate the propagation direction.

FW were first predicted as propagating velocity fluctuations confined to the fracture plane ($y=0$ plane in Figure 1a). Ramanathan and Fisher [10], building on work by Willis and Movchan [11,12], discovered that this new type of elastic wave is supported by the linearized equations describing the perturbed stress field of a moving crack. They are generated by asperities and propagate at velocities, $0.94v_R < c_f < v_R$ relative to the asperity that produced them [10,13]. Thus, the FW velocity, $c_{||}$, along the propagating front is $c_{||} = \sqrt{c_f^2 - v^2}$. FW are stable

for $\Gamma(v) = \text{const}$ and decay if $\Gamma(v)$ increases with v . FW were also observed numerically by Morrissey and Rice [13,14] and, under repeated interactions with asperities, were shown to lead to progressive roughening of the crack front profile, in agreement with previous predictions [15] of scalar models of fracture. Resonant effects of FW were anticipated in [16].

Recent experiments [17] in glass (where $\Gamma(v) \sim \text{const}$ [2]) have revealed that localized waves, whose propagation velocity corresponds to the predicted FW, are indeed emitted when a crack interacts with an asperity. The observed waves have a distinct out-of-plane (y) component which leaves traces along the fracture surface (Figure 1b). In addition, after an initial decay, observed FW rapidly converge to nondecaying long-lived waves with a unique characteristic profile (Figure 1d). FW scale is determined by the asperity size. Their *shape*, however, is independent of initial conditions. FW retain this shape upon collisions, sustaining, like solitons, a relative phase shift.

Our experiments were conducted in soda-lime glass plates of size 38x44x0.3cm in the x (propagation), y (loading) and z (sample thickness) directions, respectively (see Figure 1a). As in [18], samples were loaded using quasistatic, Mode I loading. The crack velocity was measured with a resolution of 50 m/s at the plate surfaces, i.e. the $z = 0$ and $z = 0.3\text{cm} \equiv z_{max}$ planes. Surface amplitudes were measured using a modified Taylor-Hobson (Surtronic 3+) scanning profilometer with a $0.01\mu\text{m}$ resolution normal to the fracture surface. Asperities were externally introduced within either the $z = 0$ or z_{max} planes by means of scribed lines of triangular cross-section. These lines, whose scales ranged between 100-1000 μm , locally decreased Γ . Γ was locally increased when these lines were filled with Super-glue adhesive. FW were generated by both asperity types, and above $v_c = 0.42v_R$ ($v_R = 3370\text{m/s}$) by micro-branching events. Pulse profiles (e.g. Figure 1b,c) were constructed in regions of constant mean velocity.

As Figure 1 indicates, the observed FW have a significant out-of-plane component. Do they, in addition, correspond to in-plane velocity fluctuations as predicted in [10,13,14]? To ascertain this, we measured the local velocity of the crack front on a plate face (z_{max} plane) at locations at which FW, launched from an asperity on the opposite face (the $z = 0$ plane), reached the measurement plane. The fracture surface amplitude is compared to the velocity fluctuations on this plane in Figure 2a. In Figure 2b this comparison is performed for FW generated by micro-branching events. In both cases, velocity fluctuations of 20-30% of the mean velocity correspond precisely to the arrival of the FW, as indicated by the surface height measurements. Moreover, the two signals are entirely *in phase*. These strong phase correlations are seen whenever FW are generated by externally induced asperities. These correlations are not trivial; a given velocity peak could be generated by either a surface pro-

trusion or indentation. (A protrusion on one crack face corresponds to an indentation on the other.)

We can estimate the normal velocity component $v_y \sim \delta y / \delta t$, using the surface amplitude, δy , (where $\delta t \equiv \delta x / v$ for a pulse of spatial extent δx). v_y is less than 1% of the velocity fluctuations, v_x , in the propagation direction. Thus, the relatively small out-of-plane surface (velocity) variations generated by FW correspond to large local *in-plane* fluctuations of v .

These data further indicate that FW transport significant amounts of energy along the front since, as Eq. (1) indicates, changes in v directly correspond to changes in G . This transport of energy, due to FW, explains how experiments are *able* to measure velocity fluctuations when, generally, the measurement plane at $z = 0$ or z_{max} is situated relatively far from the micro-branch events, located within the plate's interior, that initiated the fluctuations. Thus, the intrinsic velocity fluctuations measured in experiments are, in essence, front waves.

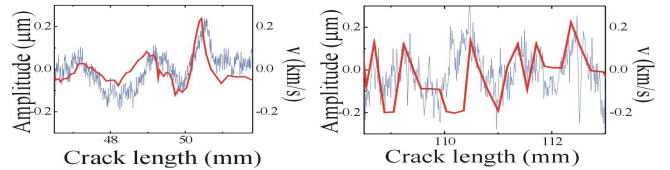


FIG. 2. Comparison, on the $z = z_{max}$ plane, of velocity fluctuations (bold line) and the fracture surface height (thin line) generated by FW for (a) FW generated by an external asperity at $v = 1000\text{m/s}$ ($0.72v_c$) (b) FW generated by micro-branching events $v = 1500\text{m/s}$ ($1.08v_c$). The velocity measurement bandwidth ($0.1\mu\text{sec} \sim 0.05 - 0.1\text{mm}$) was not sufficient to capture the fine structure of the surface measurements.

The strong correlation in both the amplitude and phase of the in-plane velocity measurements and the out-of-plane surface amplitudes indicates that these quantities can be regarded as two components of the same wave, rather than as two independent entities. These correlations suggest that significant coupling exists between in-plane and out-of-plane stress components at the crack front. As no *linear* coupling between in-plane and out-of-plane stress field components exists [12], the 3D nature of the FW is an indication of their non-linear character. A further indication of FW nonlinearity is their characteristic shape. This shape is obtained for sufficiently large perturbations [17] whereas weak perturbations generate dispersive waves that rapidly decay.

In Figure 3 we present the surface structure generated in the immediate vicinity of a single asperity that was induced at $z = 0$. In addition to the FW propagating away from the asperity, a number of additional FW are typically initiated *directly ahead* of the asperity. These additional waves indicate that the crack front immediately

ahead of the asperity retains a “memory” of the asperity’s existence. This suggests that the crack front experiences inertial effects. The highly correlated FW within these wave-trains may explain the strong phase correlations between velocity fluctuations and surface amplitudes evident in Figure 2.

The existence of these additional waves is surprising in light of the predictions of 2D fracture mechanics. As Eq. (1) indicates, a local change in the fracture energy should cause an immediate corresponding change in the instantaneous velocity of a crack. In a quasi-2D material, a crack tip can not be influenced by the stress field fluctuations generated by its interaction with an asperity. This is because stress variations radiate away [3] at the shear wave speed, c_s , which is considerably larger than v . Therefore, the moment that a crack’s tip passes an asperity’s immediate vicinity, it should instantly revert back to its initial velocity. The wave trains in Figure 3 indicate that this does not occur. The exponentially decaying amplitudes of the FW within these trains are generated *ahead* of the asperity. These FW have a well-defined period which, like their decay length ($1.8W$) and characteristic size ($\sim W$) scale ($2.3W$) with the asperity’s initial width, W .

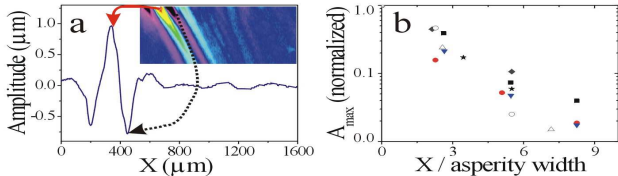


FIG. 3. (a) Profile (in the $z = 0$ plane) of a train of FW of decaying amplitude generated by a single asperity. (Asperity location is between $200\mu\text{m}$ and $400\mu\text{m}$). Note: FW are generated *ahead* of the initial asperity. (inset) Topographic map in the xz plane showing the propagating FW train. The maximum amplitudes (b) of the FW generated *ahead* of an asperity exponentially decay in the propagation direction, x , with a characteristic decay length of $1.8W$, where W is the asperity width. Values of $W = 520\mu\text{m}$ (\square), $500\mu\text{m}$ (\diamond) $430\mu\text{m}$ (∇) $410\mu\text{m}$ (\circ) $170\mu\text{m}$ (star) $160\mu\text{m}$ (open \square) and $130\mu\text{m}$ (open \triangle) were used.

What is the origin of the periodicity of the FW train? This nontrivial behavior of the crack front ahead of the asperity suggests that by breaking the system’s translational invariance along the crack front (z direction), the initially massless crack acquires inertia. A protrusion (indentation), breaking the front’s translational invariance, can influence (be influenced by) other parts of the front via stress waves. As shown in [19] (for a static crack front), the local deviation, $\delta K(z)$, of the stress field intensity from that of a straight front is proportional to:

$$\delta K(z) \propto \int_{-\infty}^{+\infty} (a(z') - a(z))/(z' - z)^2 dz' \quad (2)$$

where $(a(z') - a(z))$ is the front’s deviation in the x direction at point z along the front. The local value of $K(z)$ (the “stress intensity factor”) is proportional to $G(z)^{1/2}$ and thereby (by Eq. (1)) drives the local front velocity. Thus, any part of the front that lags (overtakes) another will experience an increased (decreased) local stress that tends to stabilize a straight front. In the dynamic case, delayed potentials will introduce inertial effects ($a(z) \Rightarrow a(z, t)$ and $K(z) \Rightarrow K(z, t)$) thereby giving rise to oscillatory behavior of the local stress field [14]. Numerical evidence for a local increase of the stress field was provided in [13], where a local increase of the front velocity was observed directly ahead of an asperity. The characteristic time scale for stress oscillations is [14] the time, W/c_{\parallel} , in which a front wave, travelling along the front with velocity $c_{\parallel} = \sqrt{c_f^2 - v^2}$, traverses an asperity of size W . Thus, the front immediately ahead of the asperity feels the effects of the oscillating stress field at a spatial scale of $Wv/c_{\parallel} = Wv/\sqrt{c_f^2 - v^2}$. This scale is consistent with the observed scaling of both the decay length (Figure 3b) and spatial periodicity (Figure 3a and Figure 4c) of the structure formed ahead of an asperity.

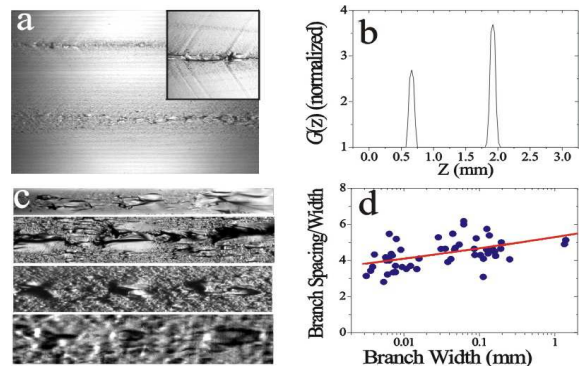


FIG. 4. (a) Photograph (of width 4mm) of two parallel branch-lines. (inset) FW emitted from a branch-line. The energy flux ($G(z)$) distribution (b) is highly non-uniform once branch-lines are formed. $G(z)$ was estimated from the fracture surface presented in (a) using measurements of micro-branch length vs micro-branch width [20]. Branch-lines are formed (c) by periodic arrays of micro-branches at many scales. Respective photograph heights are, from top to bottom, 2.4, 0.41, 0.12, and 0.03 mm. The period (d) roughly scales with the branch-line width. The predicted dependence of the branch-line period/width ratio (line) assumes that the scale in x is determined by the propagation time of a FW across the branch-line width. Crack propagation in (a) and (c) was from left to right.

Below the micro-branching instability ($v < v_c$) the surface structure described in Figure 3 is typical of that generated by the interaction of a crack front with an as-

perity. Above v_c , as shown in Figure 4, micro-branching events [17] themselves serve as FW sources since, like an asperity, they serve to increase the local value of the fracture energy. Micro-branches in glass, however, are *not* randomly dispersed throughout the fracture surface but, as shown in Figure 4a, are aligned along straight lines in the propagation direction. Their internal structure (Figure 4c,d) indicates rough periodicity in x [21]. As a consequence of the increased surface area created by the micro-branches [18] upon branch-line formation, the energy flux, G , into the front is not evenly distributed along the front. As Figure 4b shows, the total energy dissipated by a branch-line at a given location, z , along the front can be significantly larger than in the surrounding, featureless surface. This inhomogeneous distribution of G , which is perpetuated for the life of a branch-line, indicates a nonlinear focussing of energy in the z direction that is not inherent in current theories of fracture. As shown in Figure 4a, multiple “branch-lines” can co-exist, although they have a tendency to coalesce. These lines [18,21,22] are either initiated spontaneously or can be triggered by an asperity.

Let us consider the behavior of a crack front immediately after a micro-branch event/asperity of width W occurs. At the conclusion of this event the local velocity of the crack front will momentarily “overshoot” its unperturbed velocity v . For $v < v_c$, the overshoot will exponentially “ring down” as in Figure 3. For $v > v_c$ the velocity overshoot will not decay, but will instead initiate another branching event, directly ahead of the first micro-branch/asperity. This scenario will again repeat itself, thereby generating yet another branching event. In this picture, columns of branches spaced $Wv/\sqrt{c_f^2 - v^2}$ apart, in the propagation direction, will be generated. This scaling behavior is shown in Figure 4c. The initial scale, W , of the branch-lines is dynamically determined by G , as demonstrated in [18,20] where W is a roughly exponential function of v . As Figure 4d indicates, this scaling behavior is indeed observed for over 3 orders of magnitude in W . The systematic increase with v of micro-branch periodicity, apparent in the figure, is consistent with the predicted $v/\sqrt{c_f^2 - v^2}$ behavior. Note that when $v \sim v_c$ the above picture predicts that an asperity should initiate a branch-line. Slowly decaying branch-lines initiated by an asperity are indeed observed in [22] near v_c .

In conclusion, we have demonstrated that FW both transport energy along a crack front and consist of coupled in-plane and out-of-plane components. The broken translational symmetry along the front gives rise to local inertia of the front. This local inertia, when coupled to the micro-branching instability, provides a mechanism for the generation of stable, directed lines of spatially periodic micro-branches in the propagation direction. This picture, which yields an explanation of both branch-line

periodicity and scaling, may provide insight on the dynamic origins of fracture surface roughness [23]. Both the effective focussing, by branch-lines, of energy within the crack front and the spontaneous birth of local inertia within a crack front point to fundamental features of crack dynamics that cannot be incorporated in 2D descriptions of fracture.

-
- [1] H. Bergkvist, Eng. Frac. Mech. **6**, 621 (1974).
 - [2] E. Sharon and J. Fineberg, Nature **397**, 333 (1999).
 - [3] B. Q. Vu and V. K. Kinra, Eng. Frac. Mech. **15**, 107 (1981).
 - [4] L. B. Freund, *Dynamic Fracture Mechanics* (Cambridge University Press, Cambridge, 1990).
 - [5] J. D. Eshelby, Science Progress **59**, 161 (1971).
 - [6] J. Fineberg, S. Gross, M. Marder, and H. Swinney, Phys. Rev. Lett. **67**, 457 (1991).
 - [7] J. F. Boudet, S. Ciliberto, and V. Steinberg, J. Phys. II France **6**, 1493 (1996).
 - [8] T. Cramer, A. Wanner, and P. Gumbsch, Phys. Rev. Lett. **85**, 788 (2000).
 - [9] J. Fineberg and M. Marder, Physics Reports **313**, 1 (1999).
 - [10] S. Ramanathan and D. S. Fisher, Phys. Rev. Lett. **79**, 877 (1997).
 - [11] J. R. Willis and A. B. Mochvan, J. Mech. Phys. Sol. **43**, 319 (1995).
 - [12] J. R. Willis and A. B. Mochvan, J. Mech. Phys. Sol. **45**, 591 (1997); A. B. Mochvan, H. Gao, and J. R. Willis, Int. J. Sol. and Struct. **35**, 3419 (1998).
 - [13] J. W. Morrissey and J. R. Rice, J. Mech. Phys. Sol. **46**, 467 (1998).
 - [14] J. W. Morrissey and J. R. Rice, J. Mech. Phys. Sol. **48**, 1229 (2000).
 - [15] G. Perrin and J. R. Rice, J. Mech. Phys. Sol. **42**, 1047 (1994); J. R. Rice, Y. Ben-Zion, and K. S. Kim, J. Mech. Phys. Sol. **42**, 813 (1994); Y. Ben-Zion and J. W. Morrissey, J. Mech. Phys. Sol. **43**, 1363 (1995).
 - [16] J. F. Boudet and S. Ciliberto, Physica D **142**, 317 (2000).
 - [17] E. Sharon, G. Cohen, and J. Fineberg, Nature **410**, 68 (2001).
 - [18] E. Sharon and J. Fineberg, Phys. Rev. B **54**, 7128 (1996).
 - [19] J. R. Rice, J. Appl. Mech. **52**, 571 (1985).
 - [20] E. Sharon and J. Fineberg, Phil. Mag. **B78**, 243 (1998).
 - [21] E. K. Beauchamp, J. Am. Ceram. Soc. **78**, 689 (1995).
 - [22] A. Tsirk, in *Advances in ceramics: Fractography of glasses and ceramics*, edited by J. Varner and V. Frechette (The American Ceramic Society, Westerville OH, 1988), Vol. 22, pp. 57–69.
 - [23] E. Bouchaud, G. Lapasset, J. Planes, and S. Naveos, Phys. Rev. B **48**, 2917 (1993); K. J. Maloy, A. Hansen, E. L. Hinrichsen, and S. Roux, Phys. Rev. Lett. **68**, 213 (1992).